

## Radiative lifetime of the $3s3p^3(^5S_2^o)$ metastable level of $P^+$

Anthony G. Calamai, Xiaofeng Han,\* and William H. Parkinson

*Harvard-Smithsonian Center for Astrophysics, 60 Garden Street, Cambridge, Massachusetts 02138*

(Received 11 October 1991)

The radiative lifetime of the  $3s3p^3(^5S_2^o)$  metastable level of  $P^+$  has been measured by counting, for equal time intervals, the  $\sim 221$ -nm photons emitted when the metastable ions decay to the  $3s^23p^2(^3P_{2,1})$  levels of  $P^+$ . This is the first lifetime measurement of the  $3s3p^3(^5S_2^o)$  level belonging to a low-charge-state ion in the Si I isoelectronic sequence. Although forbidden to decay by the  $LS$  selection rule  $\Delta S = 0$ , the  $^5S_2^o$  level decays via intercombination electric dipole transitions by spin-orbit mixing with other levels of the  $3s3p^3$  configuration. A metastable  $P^+$  ion population was produced inside a cylindrical radio-frequency ion trap by electron bombardment of  $PH_3$  vapor at pressures ranging from  $5 \times 10^{-8}$  to  $40 \times 10^{-8}$  Torr. The trap, operated with potential-well depths ranging from 12 to 20 eV, consists of two circular, wire-mesh end caps and a cylindrical, wire-mesh ring electrode with physical dimensions  $r_0 = z_0 = 1.67$  cm. Some of the light emitted by the decaying  $^5S_2^o$  population was focused onto a 19-nm-bandwidth interference filter in front of a photomultiplier tube operated in single-photon counting mode. The mean lifetime was obtained from the decay-rate parameter of a nonlinear least-squares fit of a single exponential plus a constant background to the decay counts. Our result for the radiative lifetime of the  $3s3p^3(^5S_2^o)$  metastable level of  $P^+$  is  $167 \pm 12 \mu s$ .

PACS number(s): 32.70.Fw

### I. INTRODUCTION

A fine-structure level of an atomic ion is termed metastable if all first-order electric-dipole ( $E1$ ) matrix elements connecting the excited level to less energetic levels are zero. Of specific concern in this work is a class of metastable states that radiatively decay by intersystem or intercombination  $E1$  transitions. Intercombination transitions violate the  $LS$  selection rule  $\Delta S = 0$  and gain allowed character as the strength of the spin-orbit interaction increases with ionic charge along an isoelectronic sequence and the  $LS$ -coupling approximation gradually breaks down. Because the spin-orbit effect generally increases with nuclear charge, spin-forbidden levels of low-charge-state ions of the lighter elements have radiative lifetimes that range from microseconds [1, 2] to more than a second [3, 4], whereas similar levels of highly-ionized atoms have radiative lifetimes on the order of a few nanoseconds [5] or less [6].

Intercombination spectral lines from radiative decay of metastable levels of low-charge-state atomic ions are observed in various diffuse astrophysical [7–9] and laboratory [10, 11] plasmas. In a diffuse plasma, the rates for radiative decay—i.e., transition probabilities or  $A$  values—of metastable atomic levels can be the same order of magnitude as the rates for excitation and deexcitation by electron collisions. Intensity ratios involving lines from metastable levels are sensitive to electron densities and temperatures and are often the basis of the best diagnostic techniques [12, 13] used to determine these plasma parameters. However, the precision of these diagnostic methods critically depends on an accurate knowledge of the  $A$  values of the allowed and forbidden decays involved.

The determination of transition probabilities of intercombination transitions and radiative lifetimes of the associated spin-forbidden levels is an active area of both experimental [14, 15] and theoretical [16, 17] atomic physics research. At present,  $A$  values of the  $3s3p^3(^5S_2^o)$  metastable level of low-charge-state ions in the Si I isoelectronic sequence are quite uncertain [18, 19]. Experimentally determined radiative lifetimes for, and branching ratios of, lines from the  $^5S_2^o$  level of these ions do not exist. Moreover, the various theoretical methods [20–22] employed to calculate  $A$  values for intercombination transitions of the  $3s3p^3(^5S_2^o)$  metastable level in low-charge-state ions produced results that differ by as much as an order of magnitude. Thus precise measurements of radiative lifetimes and branching ratios for transitions from the  $^5S_2^o$  levels of these ions are required, not only to extend the available atomic physics data base, but also as essential tests of the methods employed in theoretical atomic spectroscopy [18].

We have measured the radiative lifetime of the  $3s3p^3(^5S_2^o)$  metastable level of  $P^+$  by directly observing the time dependence of photon emission from a population of  $P^+$  ( $^5S_2^o$ ) ions confined by the fields of a cylindrical radio-frequency (rf) ion trap. Figure 1 shows the position [23] of the  $P^+$  ( $^5S_2^o$ ) level relative to the fine-structure levels of the  $3s^23p^2$  ground configuration. In the Si I isoelectronic sequence, the  $^5S_2^o$  state is the least energetic level of the first excited configuration and its decay by direct- $E1$  radiation is forbidden by the  $LS$  selection rule  $\Delta S = 0$ . Thus intercombination transitions represent the dominant decay mode of the  $3s3p^3(^5S_2^o)$  metastable level. In  $P^+$ , either a 221.1- or 219.6-nm photon is emitted when the  $^5S_2^o$  state undergoes an intercombination transition to either the  $3s^23p^2(^3P_2)$  or  $^3P_1$ ) level, respectively.

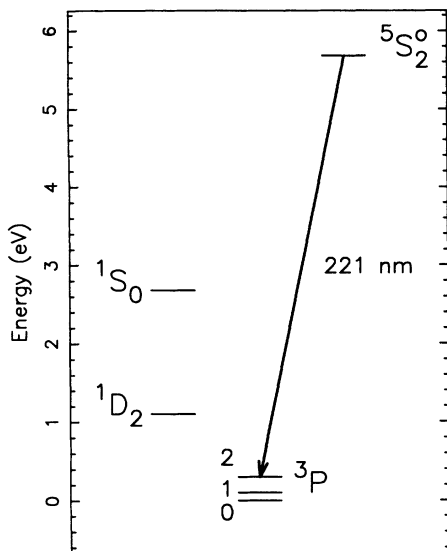


FIG. 1. Partial energy-level diagram showing the six lowest levels of  $P^+$ . The five lowest arise from the  $3s^23p^2$  ground configuration; the  $^5S_2$  state is the lowest  $3s3p^3$  configuration. The arrow indicates one of the intercombination transitions monitored for the radiative lifetime measurement of the  $^5S_2$  metastable level.

## II. EXPERIMENTAL METHOD

Ion-trapping techniques [24, 25] have greatly enhanced the accuracy with which radiative lifetimes of metastable levels of low-charge-state atomic ions can be determined. Details concerning cylindrical rf ion traps [26], and their application to metastable-state lifetime measurements [27, 28], have been discussed previously. Since the methods employed in this work differ slightly from those of previous ion-trap work in our laboratory, only a brief review of the trap and experimental method follows for completeness. The ion trap was a replica of one described by Kwong [29]. All trap electrodes were constructed of stainless-steel wire mesh. The cylindrical ring electrode with radius  $r_0 = 1.67$  cm defines the radial extent of the trap, which is axially bound by two planar end caps separated by  $2r_0$ . With the end-cap electrodes grounded and electrically insulated from the ring electrode, a time-varying voltage

$$V(t) = U_0 + V_0 \cos(\Omega t) \quad (2.1)$$

applied to the ring produces an effective potential well [24] that confines an ion population to a region bounded by the electrodes. Most of our data were collected with  $\Omega/2\pi = 686$  kHz,  $18 \leq U_0 \leq 32$  V, and  $300 \leq V_0 \leq 400$  V, yielding spherical potential wells for  $P^+$  ions that ranged from 12 to 20 eV in depth.

Production of  $P^+$  ions and excitation of the  $^5S_2$  level were accomplished inside the ion trap by electron bombardment of  $PH_3$ . The trap and a 0.1-in.-diam. tungsten dispenser cathode were located inside a vacuum chamber where the residual background pressure, as measured by a Baynard-Alpert ionization gauge, was approximately

$10^{-9}$  Torr. In order to determine if the measured lifetime showed a dependence on the pressure of the parent  $PH_3$  vapor [38], a variable-leak valve was adjusted to give stable  $PH_3$  pressures that ranged from  $5 \times 10^{-8}$  to  $40 \times 10^{-8}$  Torr. The dispenser cathode, located  $\sim 5$  mm from the top end cap of the trap and maintained at +100 V, was pulsed to  $-300$  V during the 2-ms electron bombardment interval. The electrons emitted by the cathode entered the trapping volume with about 300 eV of kinetic energy and produced various atomic and molecular fragments of the  $PH_3$  parent molecules upon impact. Cracking pattern data [30] for electron impact on  $PH_3$  indicate that approximately 12% of the fragments were  $P^+$  ions, a fraction of which were created in the  $3s3p^3(^5S_2)$  metastable state. We refer to the electron-bombardment interval as the fill period and the negative potential applied to the cathode during this period as the fill pulse. Assuming an estimated photon-counting efficiency of 0.05%, our observed signal indicates that about  $10^3$   $P^+(^5S_2)$  ions were created and stored in the trap per fill pulse. The  $P^+$  storage time—the time required for the ion population to fall to  $1/e$  of its initial value—was estimated at approximately 100 ms for a  $PH_3$  pressure of  $10^{-7}$  Torr.

After the trap was filled, some of the light emitted by the decaying metastable ion population passed through the wire-mesh ring electrode and was focused by an  $f/2$   $CaF_2$  lens onto a narrow-band interference filter positioned in front of an EMR 541F photomultiplier tube (PMT) operating in photon-counting mode. The interference filter, which had a FWHM bandwidth of about 19 nm with a 21% peak transmittance centered at 220 nm, preferentially selected photons from the  $3s3p^3(^5S_2) \rightarrow 3s^23p^2(^3P_{2,1})$  intercombination transitions and rejected unwanted background radiation predominantly emitted by thermal radiation of the dispenser cathode operating at  $\sim 1100$  °C.

Counts associated with the decay of the metastable  $^5S_2$  population were accumulated through a data collection cycle consisting of two phases; Fig. 2 represents the timing sequence used for our measurements. The rising edge of the 200-Hz, fill-pulse-logic signal triggered the start of each phase, which consists of three events: a fill pulse, a delay, and a photon-counting period. The falling edge of the fill pulse started a multichannel scaler (MCS), which was programed to insert a delay period of about  $41 \mu s$  before the beginning of the photon-counting periods. During the delay interval, the ion cloud stabilizes, and trapped ions that are created in states that are allowed to undergo  $E1$  transitions will have decayed to insignificant numbers. Photon-counting periods were programed for 128 sequential channels, each  $20.48 \mu s$  in duration, yielding a total photon-counting interval of approximately 2.6 ms per cycle. During the first phase of each cycle, the lower end cap of the trap—located on the side of the trap farthest from the dispenser cathode—was maintained at ground potential. Alternately, the second phase of each cycle had the lower end cap biased at +90 V, which effectively dumped the remaining ion population and prohibited ion storage after the second fill pulse. Thus the first photon-counting period, which corresponds to a stored  $P^+$  ion population, con-

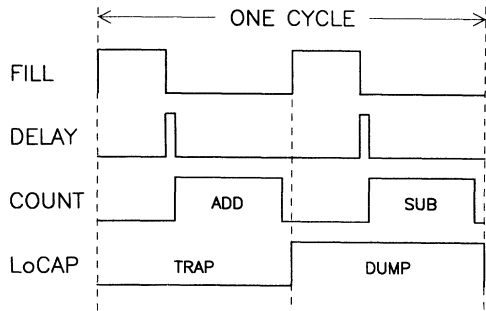


FIG. 2. Timing diagram (not to scale) of the voltage pulses applied to the ion trap during one data-collection cycle. A voltage pulse (FILL) gates on an electron beam that creates  $P^+(^5S_2^o)$  ions inside the ion trap by bombardment of  $PH_3$ . At the conclusion of the FILL interval, a multichannel scaler (MCS) inserts a 40.96- $\mu s$  delay period before the first of 128 equally spaced channels that comprise the photon-counting periods. During the first phase of each cycle, the trap end cap (LoCAP) farthest from the dispenser cathode is maintained at ground potential and the trap is tuned for  $P^+$  storage. Alternately, the second phase of each cycle has the low end cap maintained at +90 V, forbidding ion storage and dumping the remaining ions from the first phase of the data collection cycle. The second photon-counting interval collects the background counts, which are subtracted channel-by-channel from the signal-plus-background counts detected during the first half of the data collection cycle. This cycle was repeated many times to achieve signal averaging with background subtraction.

tained a record of both signal and background counts, while the second photon-counting period, with the trap detuned from ion storage, contained only background counts. Counts registered in the second counting period were subtracted from the number detected during the first period on a channel-by-channel basis and the results were added to those of previous cycles. The results of this method produced  $P^+(^5S_2^o)$  photon-decay curves with a good signal-to-noise ratio after  $4 \times 10^6$  data collection cycles. A representative decay curve for the  $3s3p^3(^5S_2^o)$  metastable level of  $P^+$  is shown in Fig. 3(a). In order to emphasize the time dependence of the decay, only the first 53 channels have been shown. Beyond this channel the curve becomes constant with the accumulated count per channel randomly distributed about zero with a mean amplitude of approximately 10 counts/channel.

### III. DATA ANALYSIS

All decay curves appeared to represent a single population, exponentially decaying into the background noise level. In order to minimize the possibility of a small, second, decay component skewing the lifetime measurements, a weighted, nonlinear, least-squares fit to the data was performed using two functional forms:

$$N(t) = N_0 e^{-\gamma t} + B, \quad (3.1)$$

where  $N_0$ ,  $\gamma$ , and  $B$  represent the respective initial population, decay rate, and background parameters of a

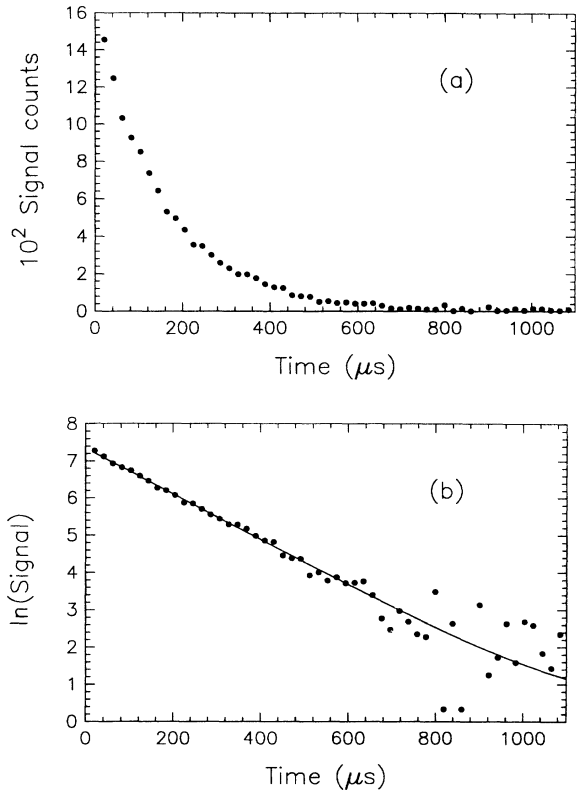


FIG. 3. (a) First 53 channels of a 128-channel decay curve of signal counts vs time as the  $3s3p^3(^5S_2^o)$  metastable level population of  $P^+$  decays. Only the first 53 channels are shown to emphasize the time dependence of the decay. An interference filter centered at 220 nm was used to monitor the  $\sim 221$ -nm photons emitted as a result of the  $(^5S_2^o \rightarrow ^3P_{2,1})$  intercombination transitions. (b) Natural logarithm of the decay curve (negative counts not shown). The solid curve represents the natural logarithm of the nonlinear least-squares fit of  $N_0 e^{-\gamma t} + B$  to the decay counts. The decay rate of the  $P^+(^5S_2^o)$  population is obtained from the decay-rate parameter  $\gamma$  of the nonlinear least-squares-fit function.

single-component decay model, and

$$N(t) = N_1 e^{-\gamma_1 t} + N_2 e^{-\gamma_2 t}, \quad (3.2)$$

where  $N_1, N_2$  and  $\gamma_1, \gamma_2$  represent the initial population and decay rate parameters of a double-component decay model. The best-fit parameters  $N_1$  and  $\gamma_1$  of the double-component fits to the data were consistent with the best-fit initial population  $N_0$  and decay rate  $\gamma$  of the single-component model. Moreover, the best-fit parameters  $N_2$  and  $\gamma_2$  indicated  $N_2 \approx B$ , and very small—occasionally negative—second-component decay rates  $\gamma_2$ . The results of this analysis confirmed that only a single component existed in the data. Finally, the reduced- $\chi^2$  statistic derived from the single-component fits to the data were consistently less than or equal to 1.0, while the reduced- $\chi^2$  statistic obtained from the double-component fits were consistently greater than 1.0. Figure 3(b) shows a logarithmic plot of the decay counts shown in Fig. 3(a); the solid curve represents the natural logarithm of the

single-component fit to the data. For each decay curve, the single-component model was fit to the decay counts over several time intervals, corresponding to channel intervals 1–128, 2–128, 4–128, 8–128, 1–96, and 1–64. No systematic dependence of the decay rate on fitting region was observed, and the decay-rate variation was within the statistical errors of the theoretical fits for each data set. Results for the background parameter  $B$  yielded values consistent with zero, while the initial population  $N_0$  showed a slight increase with  $\text{PH}_3$  pressure.

The possibility of a time-dependent background luminescence with a spectral distribution overlapping the bandpass of the interference filter is a major concern when making a direct radiative lifetime measurement of a metastable state with our technique. A time-dependent background could occur in our apparatus by either of two possible mechanisms: (1) another metastable state of stored atomic or molecular ions could decay with the emission of radiation transmitted by the interference filter, and/or (2) radiation could be produced by collisions between the stored ions and the neutral parent vapor.

Regarding the first possibility, an analysis of the energy levels [23] of the first four ionization stages of atomic phosphorous did not reveal other long-lived levels whose radiative decay would contribute undesired counts to the decay curves. We also examined data compilations [31, 32] associated with electronic transitions of the molecular ions  $\text{PH}^+$ ,  $\text{PH}_2^+$ , and  $\text{PH}_3^+$ , because the charge-to-mass ratio of these ions is amenable to storage in the trap operating with spherical-well voltages appropriate for  $\text{P}^+$  confinement. Our review indicated that electronic states of these molecular ions do not decay with the emission of radiation within the quantum efficiency envelope of the PMT used to monitor the decay of the  $\text{P}^+ (^5S_2)$  level. Thus decay radiation from other electronic states should not produce systematic effects in the present lifetime measurement.

Background luminescence created by collisions between the stored ions and the parent  $\text{PH}_3$  molecules would exhibit a time dependence reflecting the characteristic storage time of the ion population. If this effect existed in the data, it would appear as a slowly decaying component relative to the decay rate of the  $\text{P}^+ (^5S_2)$  ions. Since the parent  $\text{PH}_3$  molecules do not exhibit emission features [32] within the bandpass of the interference filter, and a slow decay component does not exist in the decay curves, radiation as a consequence of collisions between stored ions and neutral parent molecules could not result in a systematic error in the measured lifetime.

We confirmed that the decay curves accumulated with the 220-nm interference filter arose from the stored  $\text{P}^+ (^5S_2)$  population through a series of ancillary measurements. First, with a parent  $\text{PH}_3$  pressure of  $20 \times 10^{-8}$  Torr and the trap adjusted for  $\text{P}^+$  storage, the spectral response of the apparatus from 160 to 275 nm was investigated for decay radiation using a series of narrow-bandwidth interference filters. Twelve-hour signal integration times, identical to data runs collected with the 220-nm filter, were used for all test runs. Only one test run, corresponding to a filter centered at 232 nm and having approximately 3% transmittance at the  $\sim 220$ -nm

$\text{P}^+ (^5S_2)$  transition wavelengths, developed a decay curve with a signal-level approximately  $\frac{1}{7}$  that of runs accumulated with the 220-nm filter. This ratio of signal levels, between runs collected with the 232- and 220-nm filters, accurately reflected the transmittance ratio of those filters at 220 nm. Furthermore, the decay rate of the data set collected with the 232-nm filter was consistent with the measured decay rates using the 220-nm filter. All other filters used to examine the spectral response of the apparatus had zero or undetectable transmittances near 220 nm. Only flat photoresponses—i.e., a slopeless background noise level, distributed around zero—developed when these interference filters were in the experimental apparatus.

As an additional check for undesired decay radiation, the same 160–275-nm wavelength range was investigated again but without any source  $\text{PH}_3$  gas in the vacuum chamber. No decay signals were observed in any spectral band. Next, we replaced the 220-nm filter in the apparatus, reestablished a source  $\text{PH}_3$  pressure of  $20 \times 10^{-8}$  Torr, detuned the ring electrode from  $\text{P}^+$  storage, and collected a 12-h test run. This run also produced a flat photoresponse. The same flat response was obtained when the low end cap of the trap was maintained at +90 V during both add and subtract photon-counting periods of an identical test run.

The spectral response of the apparatus, coupled with the signal dependence on  $\text{PH}_3$  source molecules and the trap being tuned for  $\text{P}^+$  storage, confirm our assignment of the decay curves to the  $3s3p^3(^5S_2)$  metastable level of  $\text{P}^+$ . Other experimental parameters—such as data collection repetition rate, channel bin width, electron bombardment energy, fill-pulse duration, trap well depth, and also trap well asymmetry—were varied also to explore for possible systematic errors. The measured decay rates were always the same to within the statistical errors of the theoretical fits.

#### IV. RESULTS AND DISCUSSION

Our final measured value for the lifetime of the  $3s3p^3(^5S_2)$  metastable level of  $\text{P}^+$  is based on a total of 36 decay curves. Each required approximately 12 h to achieve a signal-to-noise ratio similar to that shown in Fig. 3(a). Eight curves were accumulated at a background  $\text{PH}_3$  pressure of  $5 \times 10^{-8}$  Torr, and seven runs were collected at each of four separate  $\text{PH}_3$  pressures ranging from  $10 \times 10^{-8}$  to  $40 \times 10^{-8}$  Torr in  $10 \times 10^{-8}$  Torr increments. Adverse effects of the  $\text{PH}_3$  source gas on the dispenser cathode prevented data collection at pressures greater than  $40 \times 10^{-8}$  Torr. As part of our effort to identify possible systematic effects, spherical-well depths ranging from 12 to 20 eV were used for decay curves collected at each  $\text{PH}_3$  pressure. Because the measured decay rates showed no systematic dependence on trap well depth, the decay rates measured at each pressure were averaged, and the mean decay rates are plotted versus  $\text{PH}_3$  pressure in Fig. 4.

The measured decay rates  $\gamma$  consist of two parts: the radiative decay rate  $\gamma_0$  plus a pressure-dependent decay

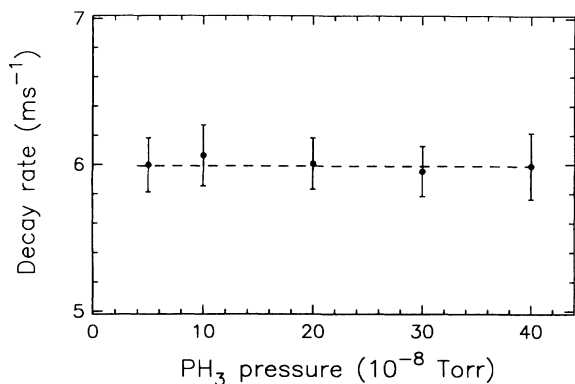


FIG. 4. Decay rates vs  $\text{PH}_3$  pressure [38] for the  $3s3p^3(^5S_2^0)$  metastable level of  $\text{P}^+$ . The dashed line represents the weighted mean of the decay rates obtained from 36 decay curves. Since no pressure dependence is observed in the measured decay rates, the natural radiative lifetime is the inverse of the mean decay rate.

rate  $\gamma_p$  that represents loss of ions in the metastable state as a consequence of collisions with the  $\text{PH}_3$  molecules present in the trapping volume. To first order in the  $\text{PH}_3$  density  $n_p$ , the measured decay rate is

$$\gamma = \gamma_0 + \gamma_p = \gamma_0 + kn_p, \quad (4.1)$$

where  $k$  is the collision-rate coefficient and  $n_p$  is the number of  $\text{PH}_3$  molecules per unit volume at a particular pressure  $P$ . However, previous ion-trap measurements [15, 33–36] of radiative lifetimes and collision-rate coefficients of metastable levels corresponding to various, low-charge-state ions indicated that the collision-rate coefficients of the various metastable ions were consistently on the order of  $10^{-9} \text{ cm}^3/\text{sec}$ . A  $\text{P}^+(^5S_2^0)$  collision rate of this magnitude would make the pressure-dependent term  $\gamma_p$  of our measured  $\text{P}^+(^5S_2^0)$  decay rates statistically insignificant relative to the radiative term  $\gamma_0$  of the decay rates. In fact, as shown in Fig. 4, the measured  $\text{P}^+(^5S_2^0)$  decay rates do not exhibit a pressure dependence. Then,  $\gamma_0 \gg \gamma_p$ , and the radiative lifetime  $\tau_0$  of the  $\text{P}^+(^5S_2^0)$  level is given by

$$\tau_0 = 1/\gamma_0 = 1/\gamma. \quad (4.2)$$

Therefore, we obtained the radiative decay rate of the  $3s3p^3(^5S_2^0)$  metastable level of  $\text{P}^+$  from a weighted average of the 36 measured decay rates. Our result for the lifetime is  $\tau_0 = 167 \pm 12 \mu\text{s}$ . Statistical errors represent the dominant source of uncertainty, but other possible errors arise from uncertainties in the MCS time-base, collisional deexcitation of the metastable state, and the time interval to which the data were fit. We estimated the sum of the uncertainties from the possible systematic effects at approximately  $\pm 4\%$  of the measured radiative lifetime. Then, by adding the total systematic uncertainty directly to the  $1\sigma$  spread of the 36 measured decay rates, we arrive at an uncertainty of 7% for our measured radiative lifetime of the  $3s3p^3(^5S_2^0)$  metastable level of  $\text{P}^+$ .

Figure 5 illustrates the results of three theoretical methods used to determine the radiative lifetime of the

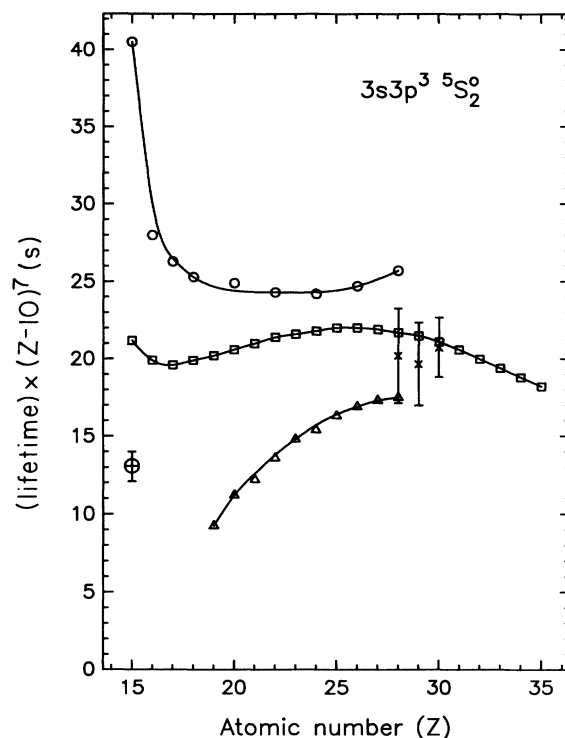


FIG. 5. Scaled mean radiative lifetime of the  $3s3p^3(^5S_2^0)$  level vs atomic number  $Z$  in the Si I isoelectronic sequence; the lifetimes are scaled by a factor of  $(Z - 10)^7$ . Theoretical results correspond to semiempirical MCHF calculations [21] ( $\circ$ ), *ab initio* MCDF calculations [20] ( $\square$ ), and semiempirical calculations using relativistic CI wave functions [22] ( $\triangle$ ). Results of beam-foil lifetime measurements [5, 37] are shown ( $\times$ ) with the reported error bars, as is the  $\text{P}^+(^5S_2^0)$  lifetime measurement reported in this work ( $\oplus$ ).

$3s3p^3(^5S_2^0)$  level in the Si I isoelectronic sequence: the semiempirical multiconfigurational Hartree-Fock MCHF [21] and the *ab initio* multiconfigurational Dirac-Fock MCDF [20] methods, and a semiempirical method using relativistic configuration-interaction CI [22] wave functions. Because the radiative lifetime of a level decaying by an intercombination transition with  $\Delta n = 0$ ,  $\Delta S = 1$  roughly scales as  $Z_c^{-7}$  [18, 20], where  $Z_c$  is the partially screened nuclear charge, the lifetimes plotted in Fig. 5 have been multiplied by a factor of  $(Z - 10)^7$ . Three beam-foil measurements [5, 37] and the result of our work for the  $3s3p^3(^5S_2^0)$  lifetime in Si-like ions are also plotted in Fig. 5.

Uncertainty estimates for the theoretical  $^5S_2^0$  lifetime results were not reported by the authors [20–22]. For the  $3s3p^3(^5S_2^0)$  level of high-charge-state ions, where *jj* coupling applies, the MCDF results should provide accurate  $A$  values and lifetimes [18]. Prior to the lifetime measurement reported in this paper, the only experimental results for the  $3s3p^3(^5S_2^0)$  lifetime corresponded to beam-foil measurements [5, 37] on  $\text{Ni}^{14+}$ ,  $\text{Cu}^{15+}$ , and  $\text{Zn}^{16+}$  ions, which confirmed the validity of the MCDF method for high-charge-state ions. However, in the case of low-charge-state species, Ellis [18] has discussed the

intractability of theoretically determining the  $3s3p^3(^5S_2^o)$  lifetime. Our measured result for the  $P^+$  ( $^5S_2^o$ ) lifetime does not agree with either of the theoretical [20, 21] results or their extrapolation [22].

Although Ellis's [21] theoretical lifetime for the  $^5S_2^o$  level of  $P^+$  is approximately 100% greater than the calculation of Huang [20], branching ratios deduced from the theoretical transition probabilities agree to about 35%. By using our measured decay rate and reported uncertainty, and adopting the average branching ratios predicted by the theoretical  $A$  values with the difference between the theoretical branching ratios serving as the error for the adopted branching ratios, we estimate the following  $A$  values for the intercombination transitions  $A(^5S_2^o \rightarrow ^3P_2) = 4629 \pm 881 \text{ s}^{-1}$  and  $A(^5S_2^o \rightarrow ^3P_1) = 1359 \pm 579 \text{ s}^{-1}$  in  $P^+$ . We hope to be able to measure the intercombination-line branching ratios in the future, so that the  $A$  values can be more accurately estimated. Ellis [18] has pointed out that such measured line strengths would lead to better spin-orbit parameters, and thus to a yardstick for improvement of the theoretical description of Si-like ions.

## V. SUMMARY

Table I summarizes the experimental and theoretical results for the radiative lifetime of the  $3s3p^3(^5S_2^o)$  metastable level of  $P^+$ . Our experimental result for the  $P^+$  ( $^5S_2^o$ ) lifetime represents the first measured lifetime of the  $3s3p^3(^5S_2^o)$  level of a low-charge-state ion in the Si I sequence. It has provided an essential test of the theoretical methods used to calculate transition probabilities for intercombination lines involving the  $3s3p^3(^5S_2^o)$  level, and indicates that the theoretical techniques used to determine such transition probabilities in low- $Z$  species of the Si I isoelectronic sequence should be reevaluated. For high-charge-state ions in the Si I isoelectronic sequence,

TABLE I. Comparison of theoretical and experimental results for the radiative lifetime  $\tau_0$  of the  $3s3p^3(^5S_2^o)$  metastable level of  $P^+$ .

| Authors                          | $\tau_0$ ( $\mu\text{s}$ ) |            |
|----------------------------------|----------------------------|------------|
| Ellis and Martinson <sup>a</sup> | 519                        | Theory     |
| Huang <sup>b</sup>               | 272                        | Theory     |
| This work                        | $167 \pm 12$               | Experiment |

<sup>a</sup>Reference [21].

<sup>b</sup>Reference [20].

the theoretical and experimental methods used to determine the lifetime of  $3s3p^3(^5S_2^o)$  level appear to give consistent results, whereas the  $^5S_2^o$  lifetimes deduced from the same theoretical techniques diverge grossly for low-charge-state species.

## ACKNOWLEDGMENTS

We thank Professor V. H. S. Kwong of UNLV for several useful discussions concerning our replica of the UNLV rf ion trap. Thanks are also extended to Professor C. E. Johnson of North Carolina State University and Dr. E. Träbert of the Ruhr-University Bochum for many useful discussions. We also acknowledge Professor Johnson for lending several interference filters used to check the photoresponse of the apparatus. We thank Dr. P. L. Smith for reading this manuscript and providing his critique of our work. Finally, we gratefully acknowledge Dr. L. D. Gardner; for without his laboratory awareness this work would have been difficult to complete. This work was supported in part by National Aeronautics and Space Administration Grant Nos NAGW-1596 and NAGW-1687 to Harvard University.

- 
- \* Present address: Department of Electrical Engineering, University of Central Florida, Orlando, FL 32816.
- [1] C. E. Johnson, *Phys. Rev. A* **5**, 2688 (1972).
- [2] H. S. Kwong, B. C. Johnson, P. L. Smith, and W. H. Parkinson, *Phys. Rev. A* **27**, 3040 (1983).
- [3] R. H. Garstang and L. J. Shamy, *Astrophys. J.* **148**, 665 (1967).
- [4] R. Glass and A. Hibbert, *J. Phys. B* **11**, 2413 (1978).
- [5] E. Träbert, *Z. Phys. D* **2**, 213 (1986).
- [6] E. Träbert, *Phys. Scr.* **41**, 625 (1990).
- [7] G. A. Doschek, U. Feldman, M. E. Van Hoosier, and J. -D. F. Bartoe, *Astrophys. J. Suppl. Ser.* **31**, 417 (1976).
- [8] H. W. Moos, S. T. Durrance, T. E. Skinner, P. D. Feldman, J. L. Bertaux, and M. C. Festou, *Astrophys. J.* **275**, L19 (1983).
- [9] K. G. Carpenter, R. F. Wing, and R. E. Stencel, *Astrophys. J. Suppl. Ser.* **57**, 405 (1985).
- [10] N. Svendenius, C. E. Magnusson, and P. O. Zetterberg, *Phys. Scr.* **27**, 339 (1983).
- [11] P. L. Smith, C. E. Magnusson, and P. O. Zetterberg, *Astrophys. J.* **277**, L79 (1984).
- [12] C. Jordan, in *Progress in Atomic Spectroscopy*, edited by W. Hanle and H. Kleinpoppen (Plenum, New York, 1979), p. 1453.
- [13] G. A. Doschek, in *Autoionization*, edited by A. Temkin (Plenum, New York, 1985), p. 175.
- [14] P. L. Smith, B. C. Johnson, H. S. Kwong, W. H. Parkinson, and R. D. Knight, *Phys. Scr.* **T8**, 8 (1984).
- [15] A. G. Calamai and C. E. Johnson, *Phys. Rev. A* **44**, 218 (1991).
- [16] A. Hibbert and D. R. Bates, *Planet. Space Sci.* **29**, 263 (1981).
- [17] P. C. Ojha, F. P. Keenan, and A. Hibbert, *J. Phys. B* **21**, L395 (1988).
- [18] D. G. Ellis, *Phys. Scr.* **40**, 12 (1989).
- [19] E. Träbert, P. H. Heckmann, R. Hutton, and I. Martinson, *J. Opt. Soc. Am. B* **5**, 2173 (1988).
- [20] K. -N. Huang, *At. Data Nucl. Data Tables* **32**, 503 (1985).
- [21] D. G. Ellis and I. Martinson, *Phys. Scr.* **30**, 255 (1984).
- [22] E. Biémont, *Phys. Scr.* **33**, 324 (1986); *J. Opt. Soc. Am. B* **3**, 163 (1986).

- [23] W. C. Martin, R. Zalubas, and A. Musgrove, *J. Phys. Chem. Ref. Data* **14**, 751 (1985), and references therein.
- [24] H. G. Dehmelt, *Adv. At. Mol. Phys.* **3**, 53 (1967); **5**, 109 (1969).
- [25] D. J. Wineland, W. M. Itano, and R. S. Van Dyck, Jr., *Adv. At. Mol. Phys.* **19**, 135 (1983).
- [26] R. F. Bonner *et al.*, *Int. J. Mass Spec. Ion Phys.* **24**, 255 (1977).
- [27] R. D. Knight, *Phys. Rev. Lett.* **48**, 792 (1982).
- [28] B. C. Johnson, P. L. Smith, and W. H. Parkinson, *Astrophys. J.* **308**, 1013 (1986).
- [29] V. H. S. Kwong, *Phys. Rev. A* **39**, 4451 (1989).
- [30] J. F. O'Hanlon, *A User's Guide to Vacuum Technology* (Wiley, New York, 1989), p. 463.
- [31] K. P. Huber and G. Herzberg, *Molecular Spectra and Molecular Structure IV: Constants of Diatomic Molecules* (Van Nostrand Reinhold, New York, 1979), p. 534, and references therein.
- [32] M. E. Jacox, *J. Phys. Chem. Ref. Data* **17** (1988), and references therein.
- [33] M. H. Prior, *Phys. Rev. A* **30**, 3051 (1984).
- [34] B. C. Johnson, P. L. Smith, and R. D. Knight, *Astrophys. J.* **281**, 477 (1984).
- [35] R. A. Walch and R. D. Knight, *Phys. Rev. A* **38**, 2375 (1988).
- [36] A. G. Calamai and C. E. Johnson, *Phys. Rev. A* **42**, 5425 (1990).
- [37] E. Träbert, P. H. Heckmann, and W. L. Wiese, *Z. Phys. D* **8**, 209 (1988).
- [38] N<sub>2</sub>-equivalent pressures are reported in this work. However, we estimate that the relative sensitivity of the Baynard-Alpert ionization gauge for PH<sub>3</sub> is within 15% of the N<sub>2</sub> standard. [See, for instance, T. D. Mark and F. Egger, *J. Chem. Phys.* **67**, 2629 (1977).]